The agreement between the mean velocity profiles computed from Eq. (11) and the experiments of Schultz-Grunow,[5] Freeman, and Klebanoff and Diehl,[8] is remarkably good at all Reynolds number values as can be seen in Fig. 4.

References

[1] Prandtl, L., "Über die Ausgebildete Turbulenz," *Zeitschrift für Angewandte Mathematik und Physik*, Vol. 5, 1925, p. 136.

[2] von Kármán, T., "Mechanische Ahnlichkeit und Turbulenz," *Proceedings of the Third International Congress on Applied Mechanics*, Vol. 1, 1931, pp. 85–93.

[3] Clauser, F. H., "Turbulent Boundary Layers in Adverse Pressure Gradient," *Journal of the Aerospace Sciences*, Vol. 21, 1954, pp. 91–108.

[4] Coles, D., "The Young Person's Guide to the Data," Air Force Office of Scientific Research Internal Flow Program Stanford Conference, 1968.

[5] Schultz-Grunow, F., "New Frictional Resistance Law for Smooth Plates," TM 986, 1941, NACA.

[6] Wieghardt, K. and Tillman, W., "On the Turbulent Friction Layer for Rising Pressure," TM 1314, 1951, NACA.

[7] Hama, F. R., "The Turbulent Boundary Layer along a Flat Plate, I and II," *Reports of the Institute of Science and Technology, University of Tokyo*, Vol. 1, 1947, pp. 13–19.

[8] Klebanoff, P. S. and Diehl, Z. W., "Some Features of Artificially Thickened Fully Developed Turbulent Boundary Layers with Zero Pressure Gradient," TN 2475, 1951, NACA.

[9] Spalding, D. B. and Chi, S. W., "The Drag of a Compressible Turbulent Boundary Layer on a Smooth Flat Plate with and without Heat Transfer," *Journal of Fluid Mechanics*, Vol. 18, Pt. 1, 1964, pp. 117–143.

[10] van Driest, E. R., "On Turbulent Flow near a Wall," *Journal of the Aerospace Sciences*, Vol. 23, 1956, pp. 1007–1011, 1036.

[11] Klebanoff, P. S., "Characteristics of Turbulence in a Boundary Layer with Zero Pressure Gradient," TR 1247, 1955, NACA.

An Experimental Study of a Yawed Circular Cone in Hypersonic Flows

Y. Y. Chan*

National Aeronautical Establishment, Ottawa, Canada

In recent years, flowfields over conical bodies can be calculated to some extent because of the advance in computational techniques. These computational methods give information on a more general condition which is no longer a small perturbation from a known flowfield at zero incidence. For a cone at incidences in a supersonic stream one may calculate the inviscid flowfield up to the relative incidence $\alpha/\theta c$ where α is the angle of attack and θc is the semiapex angle of a cone, about unity until either the cross-flow velocity component (in a spherical polar coordinate system with the cone apex at the origin) reaches supersonic locally, at which imbedded shock waves may be formed, or the vortical singularity at the leeward generator leaves the surface.[1–3] The laminar compressible boundary-layer flow over the cone surface may also be computed from the most forward generator towards the lee side of the cone until the boundary layer separates from the surface.[4–8] These methods for boundary-layer computations can be applied up to a moderate angle of attack of the cone and require only the knowledge of pressure distributions on the cone surface, provided that the vorticity interaction close to the most windward generator is small and negligible.

The aim of the present work is to determine experimentally some flow quantities, such as static pressure distributions, heat-transfer distributions, and flow directions on the surface of a cone at moderate angle of attack. From these results the range of application of these advanced methods of computation for both inviscid and boundary-layer flows are assessed.

Received March 12, 1969; revision received June 30, 1969.

* Associate Research Officer, High Speed Aerodynamics Section. Member AIAA.

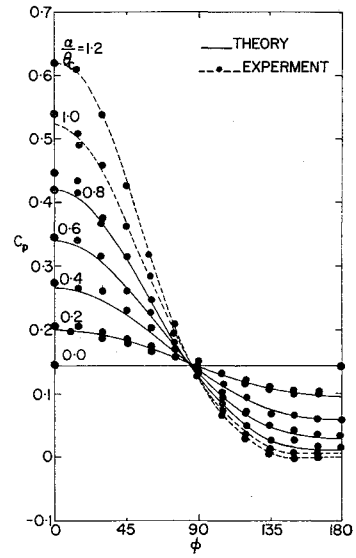

Fig. 1 Pressure distributions on a 15° circular cone at $M_\infty = 10.4$, $Re_{\infty x} = 10^6$.

Experimental Methods

Measurements were made on a right circular cone with a semiapex angle of 15°. The model is 4 in. long and the measuring station is located at $3\frac{1}{2}$ in. away from the apex so that the effect of self-induced pressure interaction at hypersonic speed is negligible at the present testing condition. The pressure measurements were made by small variable reluctance pressure transducers located inside the model as close as possible to the measuring holes. The heat-transfer measurements were made by heat-transfer gages of thin film thermometer type placed along the cone generator. The oil dots technique was used for surface flow visualization. The directions of the surface flow were then measured from the flow patterns.

The experiments were performed in the National Aeronautical Establishment hypersonic gun tunnel. The Mach number in the test section was 10.4 and the Reynolds number was 3.7×10^6/ft. The wall-to-stagnation temperature ratio was 0.23 and the boundary layers were laminar for these conditions. The model was pitched at relative incidences up to 1.2 with 0.2 steps. Surface pressure and heat-transfer distributions were measured at 15° circumferential angle steps around the cone.

Results and Discussion

With the assumption of high Reynolds number flow, the theoretical results for the inviscid and the viscous flows could be computed separately. The inviscid flowfields were calculated by the method of Ref. 3 for different relative incidences until local supersonic crossflow occurred (at $\alpha/\theta c$ about unity for the present conditions). The resulting pressure distributions from the inviscid flow model were then used to compute the boundary-layer flows by the method of Ref. 7.

The pressure distributions on the cone surface at different relative incidences are shown in Fig. 1. The over-all agreement between the computed pressure distributions and the experimental results is very good. At relative incidences of 0.6 and 0.8, the measured pressure is slightly higher than the theoretical curve at the circumferential angle ϕ near and at 180° (where ϕ is measured from the most windward generator of the cone). This is due to the piling up of vortical fluid in this region and to the displacement of the viscous flow effectively changing the local pressure distribution as observed in Refs. 9 and 10. At $\alpha/\theta c = 0.8$, the pressure minimum starts

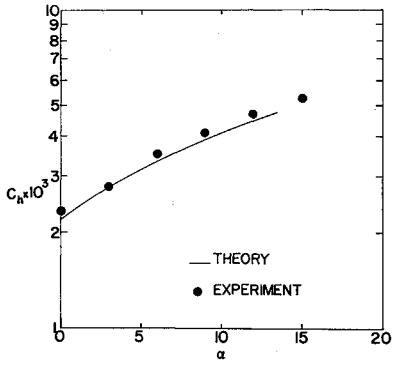

Fig. 2 Heat-transfer coefficient (Stanton number) at the most windward generator on a 15° circular cone at $M_\infty = 10.4$, $Re_{\infty x} = 10^6$.

to move away from $\phi = 180°$. The boundary-layer flow will then encounter an adverse pressure gradient and may consequently separate from the cone surface. The pressure measurements for $\alpha/\theta c$ of 1.0 and 1.2 show features of separations on the lee side as relatively large recompressions occur beginning at about $\phi = 150°$. No theoretical results are shown for these two cases as the method fails because of occurrence of local supersonic cross flow.

To compute the boundary layer along the most windward generator of the cone, $\phi = 0$, an exact method is available.[11] The comparison between the theoretical and experimental results is shown in Fig. 2 and the agreement is excellent. The theoretical results are corrected for Prandtl number of 0.7.

Away from the most windward generator, the boundary layer on the cone is computed by the small cross-flow theory[7] and the results for different relative incidences are shown in Fig. 3. The agreement between the theoretical and the experimental results are excellent for most of the surface. At $\alpha/\theta c$ of 0.4 and 0.6, the measured values of heat transfer are lower than the theoretical curve starting at $\phi = 150°$. This is due to the fact that the viscous fluid in the boundary layer is swept into this region and induces lower heat transfer to the body. At $\alpha/\theta c = 0.8$, the experiment results show that the heat transfer at $\phi = 180°$ starts to recover and this trend continued to higher values of $\alpha/\theta c$. At $\alpha/\theta c$ of 1.0 and 1.2, the heat-transfer minimums have moved away from $\phi = 180°$. This indicates that there is an outflow of the boundary layer away from the most leeward generator towards the pressure minima at both sides of the cone.

The surface flow angle ω, relative to the local generator of the cone as measured from the flow visualization experiment,

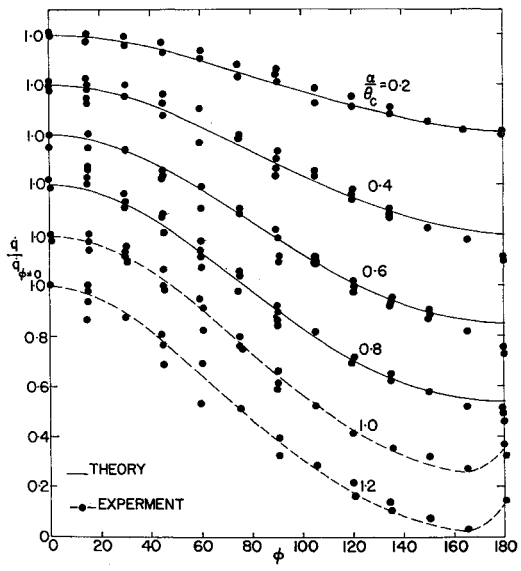

Fig. 3 Heat-transfer distributions on a 15° circular cone at $M_\infty = 10.4$, $Re_{\infty x} = 10^6$.

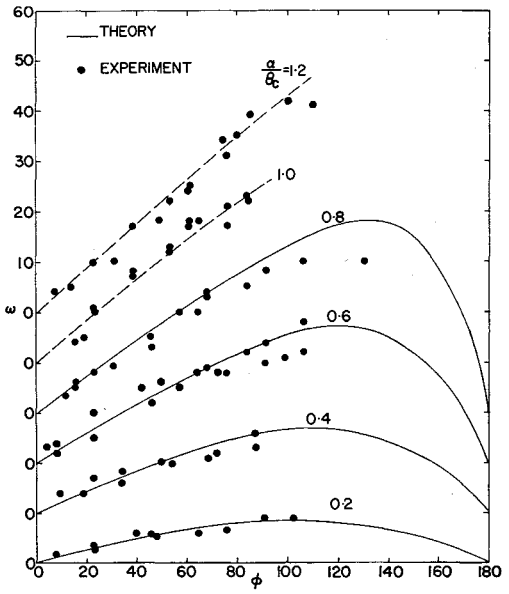

Fig. 4 Surface flow directions on a 15° circular cone at $M_\infty = 10.4$, $Re_{\infty x} = 10^6$.

are shown in Fig. 4 in comparison with theoretical results. The agreement is quite good in view of the scattering of the measured results. After a certain circumferential angle at the leeward side of the cone, the surface shear stress was so low that the oil dots did not flow at all. Thus one was unable to obtain measurements at that portion of the cone surface and to estimate the separation position of the boundary layer near the most leeward generator.

From this comparison, we may observe that the theoretical methods for calculating inviscid conical flow are highly accurate and valid on most of the cone except where the boundary-layer displacement effect is so large that the body shape is effectively changed as in the region close to the most leeward generator of the cone. The boundary-layer flows along the most windward generator and away from the plane of symmetry are well predicted by the theoretical methods except again in the aforementioned region in which the piling up of vortical fluid or even flow separation occurs.

References

[1] Babenko, K. I., "Three-dimensional Flow of Ideal Gas past Smooth Bodies," TT F-380, 1966, NASA.

[2] Moretti, G., "Inviscid Flow Field Past a Point Cone at an Angle of Attack. Part I—Analysis," TR 577, Dec. 1965, General Applied Science Lab. Inc., Westbury, N. Y.

[3] Jones, D. J., "Numerical Solutions of Flow Field for Conical Bodies in a Supersonic Stream," Aeronautical Report LR-507, July 1968, National Research Council of Canada.

[4] Tsen, L. F., "Contribution a l'Etude de la Couche Limite Tridimensionnelle Laminaire Compressible avec Transfert de Chaleur," Publications Scientifiques et Techniques No. 435, April 1967, Ministère de l'Air, France.

[5] Chan, Y. Y., "An Approximate Method for Three-Dimensional Compressible Laminar Boundary Layers with Small Cross-Flow," Aeronautical Report LR-455, June 1966, National Research Council of Canada.

[6] Fannelop, T. K., "A Method of Solving the Three-dimensional Laminar Boundary Layer Equations with Application to the Lifting Re-Entry Body," *AIAA Journal*, Vol. 6, No. 6, June 1968, pp. 1075–1084.

[7] Tsen, L. F. and Arnandon, J. F., "Couche Limite Laminaire Compressible sur une Surface Conique," *Proceedings of the Canadian Congress of Applied Mechanics*, Vol. 2, Université Laval, Quebec, Canada, May 1967, pp. 20, 206–208.

[8] Cooke, J. C., "Supersonic Laminar Boundary Layers on Cones," TR 66347, Nov. 1966, Royal Aircraft Establishment, U.K.

[9] Tracy, R. R., "Hypersonic Flow over Yawed Circular Cone," Hypersonic Research Project Memo 69, Aug. 1963,

Graduate Aeronautical Lab., California Institute of Technology, Pasadena, Calif.

[10] Feldhuln, R. H. and Pasiuk, L., "An Experimental Investigation of the Aerodynamic Characteristics of Slender Hypersonic Vehicles at High Angle of Attack," NOLTR 68-52, May 1968, U. S. Naval Ordnance Lab.

[11] Reshotko, E., "Laminar Boundary Layer with Heat Transfer on a Cone at Angle of Attack in a Supersonic Stream," TN 4152, 1957, NACA.

Hypersonic Boundary-Layer Transition on Ablating and Nonablating Cones

MICHAEL C. FISCHER*
NASA Langley Research Center, Hampton, Va.

Introduction

IN the design of re-entry vehicles, effects of the ablating protective heat shield on the vehicle flowfield are especially important with high-performance, slender configurations. Mass transpiration, nose shape changes, and surface roughness are a few of the parameters that can alter the location of natural boundary-layer transition, thus affecting the local surface heat transfer and vehicle aerodynamic characteristics. Recent results of investigations dealing with boundary-layer transition on ablating cones are given in Ref. 1–4, but limited data exist concerning actual magnitudes of reductions in the transition Reynolds number due to ablation. Here, we present preliminary results from an experimental investigation conducted to determine the effect of ablation on transition on slender cones at a nominal Mach number of 7.

Discussion

The ablating models used in this investigation were 10° half-angle cones with an axial length of 12 in., composed of paradichlorobenzene ($C_6H_4Cl_2$), which is a low-temperature subliming material with uniform ablation rates. A sharp stainless-steel nose tip prevented blunting and maintained "sharp cone" conditions at the boundary-layer edge. The ablating models were identical in initial external geometry to the nonablating model that was instrumented with thermocouples for heat-transfer measurements.

The investigation was conducted in the Langley 11-in. hypersonic tunnel. Tunnel stagnation pressure varied from 185 psia to 609 psia for a range of freestream unit Reynolds numbers of 1.68×10^6–6.21×10^6/ft. For the ablating models, tunnel stagnation temperature was about 1280°R, whereas for the metal model, tests were conducted at stagnation temperatures of about 1055° and 1280°R, giving a slight variation in the ratio T_w/T_t in order to assess the effect of these small changes in tunnel conditions on boundary-layer transition. The freestream Mach number was between 6.82 and 6.88 depending on unit Reynolds number.

Results

Transition was determined from Stanton number distributions for the metal nonablating model, and by surface recession measurements for the ablating models. The beginning of transition for the metal model was the surface location where the Stanton numbers began to deviate from laminar theory, and the end of transition was taken as the peak Stanton number. For the ablating model, surface recession was measured at three peripheral locations about each ablated model,

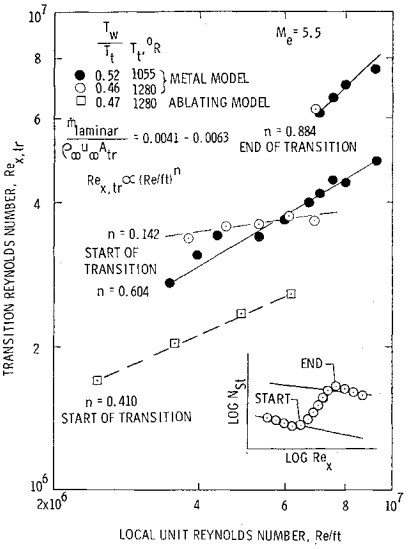

Fig. 1 Effect of mass addition on transition Reynolds number on a slender cone.

ϕ = 0°, 90°, and 180°, with the start of transition taken as the location where surface recession began to increase from the measured laminar value. There was no significant unsymmetrical transition observed so the average of the three readings was taken as the transition location.

Transition Reynolds numbers for both the metal cone and the ablating cones are presented in Fig. 1. Transition Reynolds numbers for the ablating cones were about 30–40% lower than those for the metal cone for nondimensional mass ablation rates of $\dot{m}_{laminar}/\rho_\infty u_\infty A_{tr}$ = 0.0041 to 0.0063. In this expression $\dot{m}_{laminar}$ represents the amount of mass injected into the laminar boundary layer and A_{tr} is the cross-sectional area of the cone at the start of transition. As a comparison, results from Ref. 4 on an 8° half-angle ablating cone ($C_6H_4Cl_2$) at M_∞ = 10 and with $\dot{m}_{laminar}/\rho_\infty u_\infty A_{tr}$ = 0.0070 to 0.0076 indicate a 6–12% reduction in transition Reynolds number.

In the present ablation tests, a rearward facing step was formed at the interface of the ablation material and the nonablating steel tip. The maximum value of this step (end of test run) was about 0.040 in. However, this step was not believed to influence transition significantly based on studies in Ref. 3 with oversized tips on a metal cone model at nearly the same local Mach number as in the present experiment. For Larson's tests the rearward facing step was 0.05–0.10 in. and the transition Reynolds number was reduced a maximum of 10%. In addition, unpublished data obtained by Stainback at Langley on a 5° half-angle slightly blunted cone at M_∞ = 8 with a rearward facing step of 0.040 in. indicate no noticeable effect of the step on transition over a local Mach number range of 3.7–6.3. The effect of these steps on transition is more pronounced in the lower supersonic Mach number range, as noted in Ref. 5.

The unit Reynolds number effect on transition varied from weak to strong for the ablating and nonablating transition Reynolds numbers. From the faired lines through the data, power-law relations of the form $Re_{x,tr} = C(Re/\text{ft})^n$ were calculated. The resulting values of the power-law exponent were n = 0.410 for the ablating cones at T_w/T_t = 0.47 (start of transition), n = 0.142 for the metal cone at T_w/T_t = 0.46 (start of transition), n = 0.604 for the metal cone at T_w/T_t = 0.52 (start of transition), and n = 0.884 for the metal cone at T_w/T_t = 0.52 (end of transition).

Considering the metal cone data separately, the transition Reynolds numbers were less sensitive to local unit Reynolds number for T_w/T_t = 0.46 (T_t = 1280°R) as indicated by the n = 0.142 power-law exponent. The normal method of varying the wall temperature ratio is to cool the model internally,

Received May 19, 1969; revision received July 3, 1969.
* Aero-Space Technologist, Aero-Physics Division.